An Experimental Study of Algorithms for Geodesic Shortest Paths in the Constant-Workspace Model*

Jonas Cleve[0000−0001−8480−1726] and Wolfgang Mulzer[0000−0002−1948−5840]

Institut für Informatik, Freie Universität Berlin, Takustr. 9, 14195 Berlin, Germany
[jonascleve, mulzer]@inf.fu-berlin.de

Abstract. We perform an experimental evaluation of algorithms for finding geodesic shortest paths between two points inside a simple polygon in the constant-workspace model. In this model, the input resides in a read-only array that can be accessed at random. In addition, the algorithm may use a constant number of words for reading and for writing. The constant-workspace model has been studied extensively in recent years, and algorithms for geodesic shortest paths have received particular attention.
We have implemented three such algorithms in Python, and we compare them to the classic algorithm by Lee and Preparata that uses linear time and linear space. We also clarify a few implementation details that were missing in the original description of the algorithms. Our experiments show that all algorithms perform as advertised in the original works and according to the theoretical guarantees. However, the constant factors in the running times turn out to be rather large for the algorithms to be fully useful in practice.

Keywords: simple polygon · geodesic shortest path · constant workspace · experimental evaluation

1 Introduction

In recent years, the *constant-workspace model* has enjoyed growing popularity in the computational geometry community [6]. Motivated by the increasing deployment of small devices with limited memory capacities, the goal is to develop simple and efficient algorithms for the situation where little workspace is available. The model posits that the input resides in a read-only array that can be accessed at random. In addition, the algorithm may use a constant number of memory words for reading and for writing. The output must be written to a write-only memory that cannot be accessed again for reading. Following the initial work by Asano *et al.* from 2011 [2], numerous results have been published for this model, leading to a solid theoretical foundation for dealing with geometric problems when the working memory is scarce. The recent survey by Banyassady *et*

* Supported in part by DFG projects MU/3501-1 and RO/2338-6 and ERC StG 757609.

al. [6] gives an overview of the problems that have been considered and of the results that are available for them.

But how do these theoretical results measure up in practice, particularly in view of the original motivation? To investigate this question, we have implemented three different constant-workspace algorithms for computing geodesic shortest paths in simple polygons. This is one of the first problems to be studied in the constant-workspace model [2,3]. Given that the general shortest path problem is unlikely to be amenable to constant-workspace algorithms (it is NL-complete [18]), it may come as a surprise that a solution for the geodesic case exists at all. By now, several algorithms are known, both for constant workspace as well as in the *time-space-trade-off* regime, where the number of available cells of working memory may range from constant to linear [1,12].

Due to the wide variety of approaches and the fundamental nature of the problem, geodesic shortest paths are a natural candidate for a deeper experimental study. Our experiments show that all three constant-workspace algorithms work well in practice and live up to their theoretical guarantees. However, the large running times make them ill-suited for very large input sizes. During our implementation, we also noticed some missing details in the original publications, and we explain below how we have dealt with them.

As far as we know, our study constitutes the first large-scale comparative evaluation of geometric algorithms in the constant-workspace model. A previous implementation study, by Baffier *et al.* [5], focused on time-space trade-offs for stack-based algorithms and was centered on different applications of a powerful algorithmic technique. Given the practical motivation and wide applicability of constant-workspace algorithms for geometric problems, we hope that our work will lead to further experimental studies in this direction.

2 The Four Shortest-Path Algorithms

We provide a brief summary for each of the four algorithms in our implementation; further details can be found in the original papers [3,2,14]. In each case, we use P to denote a simple input polygon in the plane with n vertices. We consider P to be a closed, connected subset of the plane. Given two points $s, t \in P$, our goal is to compute a shortest path from s to t (with respect to the Euclidean length) that lies completely inside P.

2.1 The Classic Algorithm by Lee and Preparata

This is the classic linear-space algorithm for the geodesic shortest path problem that can be found in textbooks [14,11]. It works as follows: we triangulate P, and we find the triangle that contains s and the triangle that contains t. Next, we determine the unique path between these two triangles in the dual graph of the triangulation. The path is unique since the dual graph of a triangulation of a simple polygon is a tree [7]. We obtain a sequence $e_1, \ldots, e_m$ of diagonals (incident to pairs of consecutive triangles on the dual path) crossed by the geodesic shortest

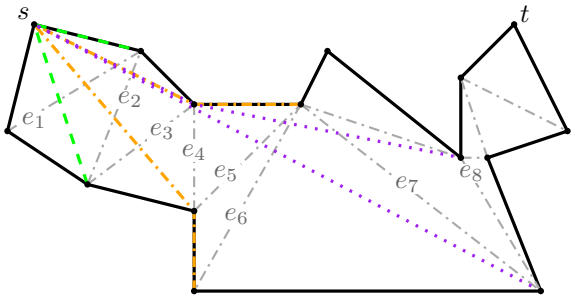

Fig. 1: Examples of three funnels during the algorithm for finding a shortest path from s to t. Each has cusp s and goes up to diagonals e_2 (green, dashed), e_6 (orange, dash dotted), and e_8 (purple, dotted).

path between s and t, in that order. The algorithm walks along these diagonals, while maintaining a *funnel*. The funnel consists of a *cusp* p, initialized to be s, and two concave *chains* from p to the two endpoints of the current diagonal e_i. An example of these funnels can be found in Fig. 1. In each step i of the algorithm, $i = 1, \ldots, m-1$, we update the funnel for e_i to the funnel for e_{i+1}. There are two cases: (i) if e_{i+1} remains visible from the cusp p, we update the appropriate concave chain, using a variant of Graham's scan; (ii) if e_{i+1} is no longer visible from p, we proceed along the appropriate chain until we find the cusp for the next funnel. We output the vertices encountered along the way as part of the shortest path. Implemented in the right way, this procedure takes linear time and space.[1]

2.2 Using Constrained Delaunay-Triangulations

The first constant-workspace-algorithm for geodesic shortest paths in simple polygons was presented by Asano *et al.* [3] in 2011. It is called *Delaunay*, and it constitutes a relatively direct adaptation of the method of Lee and Preparata to the constant-workspace model.

In the constant-workspace model, we cannot explicitly compute and store a triangulation of P. Instead, we use a uniquely defined implicit triangulation of P, namely the *constrained Delaunay triangulation* of P [9]. In this variant of the classic Delaunay triangulation, we prescribe the edges of P to be part of the desired triangulation. Then, the additional triangulation edges cannot cross the prescribed edges. Thus, unlike in the original Delaunay triangulation, the circumcircle of a triangle may contain other vertices of P, as long as the line segment from a triangle endpoint to the vertex crosses a prescribed polygon edge, see Fig. 2 for an example.

[1] If a triangulation of P is already available, the implementation is relatively straightforward. If not, a linear-time implementation of the triangulation procedure constitutes a significant challenge [8]. Simpler methods are available, albeit at the cost of a slightly increased running time of $O(n \log n)$ [7].

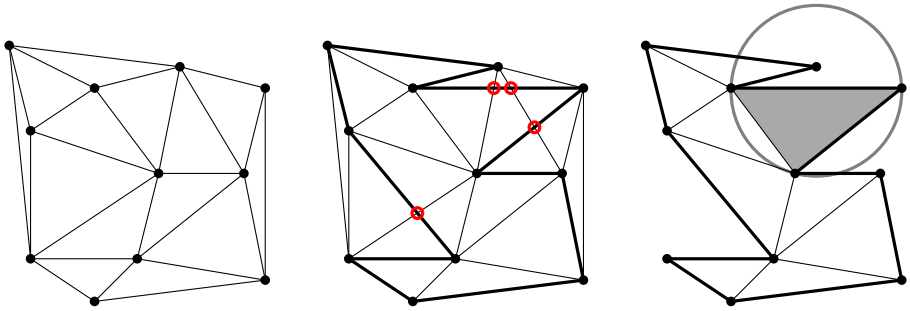

(a) The Delaunay triangulation of a point set.

(b) A polygon on the point set which intersects the triangulation.

(c) The circumcircle may contain points not visible from some triangle vertices.

Fig. 2: An example of a constrained Delaunay triangulation of a simple polygon.

The constrained Delaunay triangulation of P can be navigated efficiently using constant workspace: given a diagonal or a polygon edge, we can find the two incident triangles in $O(n^2)$ time [3]. Using an $O(n)$ time constant-workspace-algorithm for finding shortest paths in trees, also given by Asano *et al.* [3], we can thus enumerate all triangles in the dual path between the constrained Delaunay triangle that contains s and the constrained Delaunay triangle that contains t in $O(n^3)$ time.

As in the algorithm by Lee and Preparata, we need to maintain the visibility funnel while walking along the dual path of the constrained Delaunay triangulation. Instead of the complete chains, we store only the two line segments that define the current visibility cone (essentially the cusp together with the first vertex of each chain). We recompute the two chains whenever it becomes necessary. The total running time of the algorithm is $O(n^3)$. More details can be found in the paper by Asano *et al.* [3].

2.3 Using Trapezoidal Decompositions

This algorithm was also proposed by Asano *et al.* [3], as a faster alternative to the algorithm that uses constrained Delaunay triangulations. It is based on the same principle as *Delaunay*, but it uses the trapezoidal decomposition of P instead of the Delaunay triangulation [7]. See Fig. 3 for a depiction of the decomposition and the symbolic perturbation method to avoid a general position assumption. In the algorithm, we compute a trapezoidal decomposition of P, and we follow the dual path between the trapezoid that contains s and the trapezoid that contains t, while maintaining a funnel and outputting the new vertices of the geodesic shortest path as they are discovered. Assuming general position, we can find all incident trapezoids of the current trapezoid and determine how to continue on the way to t in $O(n)$ time (instead of $O(n^2)$ time in the case of the *Delaunay* algorithm). Since there are still $O(n)$ steps, the running time improves to $O(n^2)$.

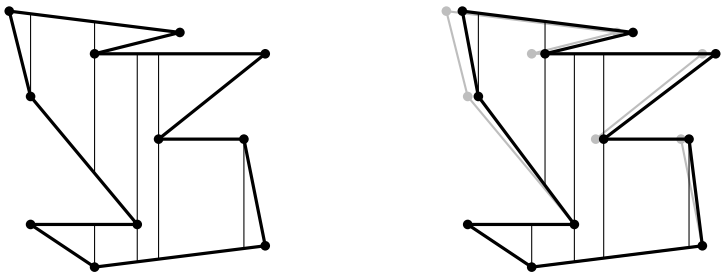

(a) The trapezoidal decomposition is obtained by shooting rays up and down at every vertex.

(b) Shifting all points to the right by $y\varepsilon$ makes sure no two share the same x-coordinate.

Fig. 3: The trapezoidal decomposition of a polygon. If the polygon is in general position (right) each trapezoid has at most four neighbors which can all be found in $O(n)$ time.

2.4 The Makestep Algorithm

This algorithm was presented by Asano *et al.* [2]. It uses a direct approach to the geodesic shortest path problem and unlike the two previous algorithms, it does not try to mimic on the algorithm by Lee and Preparata. In the traditional model, this approach would be deemed too inefficient, but in the constant-workspace world, its simplicity turns out to be beneficial. The main idea is as follows: we maintain a *current vertex* p of the geodesic shortest path, together with a *visibility cone*, defined by two points q_1 and q_2 on the boundary of P. The segments pq_1 and pq_2 cut off a subpolygon $P' \subseteq P$. We maintain the invariant that the target t lies in P'. In each step, we gradually shrink P' by advancing q_1 and q_2, sometimes also relocating p and outputting a new vertex of the geodesic shortest path. These steps are illustrated in Fig. 4. It is possible to realize the shrinking steps in such a way that there are only $O(n)$ of them. Each shrinking step takes $O(n)$ time, so the total running time of the MakeStep algorithm is $O(n^2)$.

3 Our Implementation

We have implemented the four algorithms from Section 2 in Python [15]. For graphical output and for plots, we use the `matplotlib` library [13]. Even though there are some packages for Python that provide geometric objects such as line segments, circles, etc., none of them seemed suitable for our needs. Thus, we decided to implement all geometric primitives on our own. The source code of the implementation is available online in a Git-repository.[2]

In order to apply the algorithm *Lee-Preparata*, we must be able to triangulate the simple input polygon P efficiently. Since implementing an efficient polygon

[2] https://github.com/jonasc/constant-workspace-algos

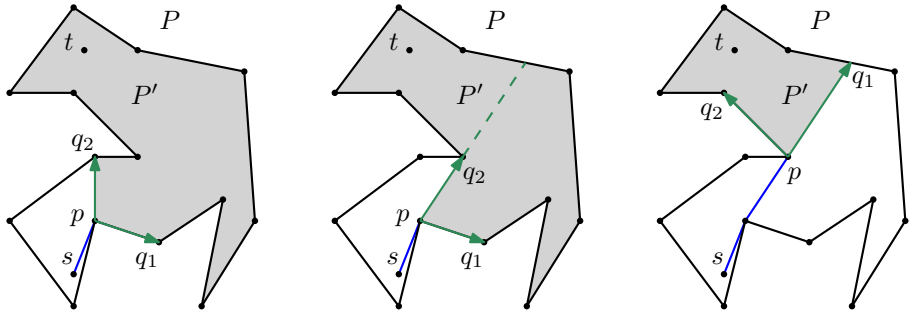

(a) P' is the subset of P cut off by the three points p, q_1, and q_2. Both points are convex, one is advanced.

(b) Since q_2 is reflex we shoot a ray until it hits the boundary. t lies to the left of this ray.

(c) p is relocated to the previous position of q_2 and P' is shrunk along the ray.

Fig. 4: An illustration of the steps in the *Makestep* algorithm.

triangulation algorithm can be challenging and since this is not the main objective of our study, we relied for this on the *Python Triangle* library by Rufat [16], a Python wrapper for Shewchuk's *Triangle*, which was written in C [17]. We note that *Triangle* does not provide a linear-time triangulation algorithm, which would be needed to achieve the theoretically possible linear running time for the shortest path algorithm. Instead, it contains three different implementations, namely Fortune's sweep line algorithm, a randomized incremental construction, and a divide-and-conquer method. All three implementations give a running time of $O(n \log n)$. For our study, we used the divide-and conquer algorithm, the default choice. In the evaluation, we did not include the triangulation phase in the time and memory measurement for running the algorithm by Lee and Preparata.

3.1 General Implementation Details

All three constant-workspace algorithms have been presented with a general position assumption: *Delaunay* and *Makestep* assume that no three vertices lie on a line, while *Trapezoid* assumes that no two vertices have the same x-coordinate. Our implementations of *Delaunay* and *Makestep* also assume general position, but they throw exceptions if a non-recoverable general position violation is encountered. Most violations, however, can be dealt with easily in our code; e.g. when trying to find the constrained Delaunay triangle(s) for a diagonal, we can simply ignore points collinear to this diagonal. For the case of *Trapezoid*, Asano *et al.* [3] described how to enforce the general position assumption by changing the x-coordinate of every vertex to $x + \varepsilon y$ for some small enough $\varepsilon > 0$ such that the x-order of all vertices is maintained. In our implementation, we apply this method to every polygon in which two vertices share the same x-coordinate.

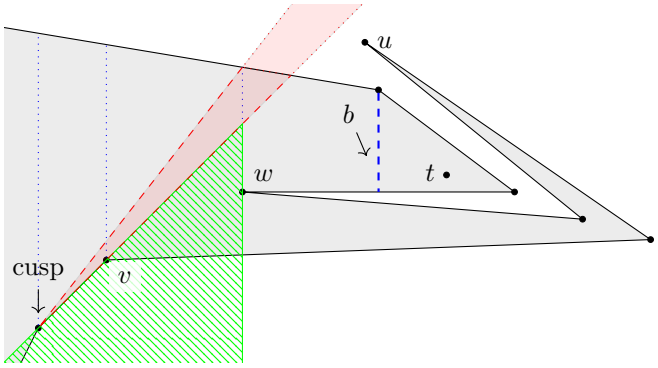

Fig. 5: During the gift wrapping from the cusp to the diagonal b, the vertices need to be restricted to the shaded area. Otherwise, u would be considered to be part of the geodesic shortest path, as it is to the left of vw.

The coordinates are stored as 64 bit IEEE 754 floats. In order to prevent problems with floating point precision or rounding, we take the following steps: first, we never explicitly calculate angles, but we rely on the usual three-point-orientation test, i.e., the computation of a determinant to find the position of a point c relative to the directed line through to points a and b [7]. Second, if an algorithm needs to place a point somewhere in the relative interior of a polygon edge, we store an additional edge reference to account for inaccuracies when calculating the new point's coordinates.

3.2 Implementing the Algorithm by Lee and Preparata

The algorithm by Lee and Preparata can be implemented easily, in a straightforward fashion. There are no particular edge cases or details that we need to take care of. Disregarding the code for the geometric primitives, the algorithm needs less then half as many lines of code than the other algorithms.

3.3 Implementing Delaunay and Trapezoid

In both constant-workspace adaptations of the algorithm by Lee and Preparata, we encounter the following problem: whenever the cusp of the current funnel changes, we need to find the cusp of the new funnel, and we need to find the piece of the geodesic shortest path that connects the former cusp to the new cusp. In their description of the algorithm, Asano *et al.* [3] only say that this should be done with an application of gift wrapping (Jarvis' march) [7]. While implementing these two algorithms, we noticed that a naive gift wrapping step that considers all the vertices on P between the cusp of the current funnel and the next diagonal might include vertices that are not visible inside the polygon. Figure 5 shows an example: here b is the next diagonal, and naively we would look at all vertices along the polygon boundary between v and w. Hence, u would be

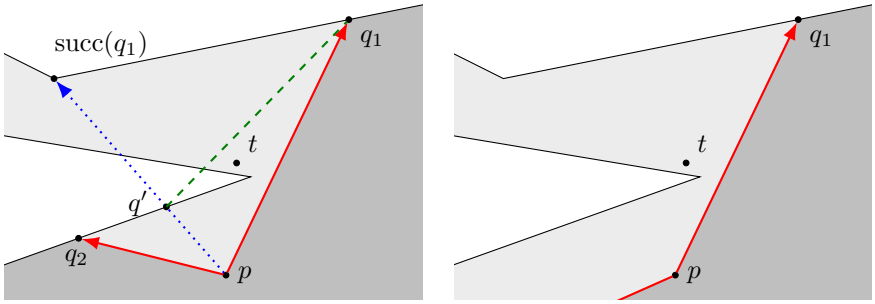

Fig. 6: Left: Asano *et al.* [2] state that one should check whether "t lies in the subpolygon from q' to q_1." This subpolygon, however, is not clearly defined as the line segment $q'q_1$ does not lie inside P. Considering pq' instead and using q_1pq' to shrink the cutoff region gives the correct result on the right.

considered as a gift wrapping candidate, and since it forms the largest angle with the cusp and v (in particular, an angle that is larger than the angle formed by w) it would be chosen as the next point, even though w should be the cusp of the next funnel. A simple fix for this problem would be an explicit check for visibility in each gift-wrapping step. Unfortunately, the resulting increase in the running time would be too expensive for a realistic implementation of the algorithms.

Our solution for *Trapezoid* is to consider only vertices whose x-coordinate is between the cusp of the current vertex and the point where the current visibility cone crosses the boundary of P for the first time. For ease of implementation, one can also limit it to the x-coordinate of the last trapezoid boundary visible from the cusp. Figure 5 shows this as the dotted green region. For *Delaunay*, a similar approach can be used. The only difference is that the triangle boundaries in general are not vertical lines.

3.4 Implementing Makestep

Our implementation of the *Makestep* algorithm is also relatively straightforward. Nonetheless, we would like to point out one interesting detail; see Fig. 6. The description by Asano *et al.* [2] says that to advance the visibility cone, we should check if "*t lies in the subpolygon from q' to q_1*." If so, the visibility cone should be shrunk to $q'pq_1$, otherwise to q_2pq'.

However, the "*subpolygon from q' to q_1*" is not clearly defined for the case that the line segment $q'q_1$ is not contained in P. To avoid this difficulty, we instead consider the line segment pq'. This line segment is always contained in P, and it divides the cutoff region P' into two parts, a "subpolygon" between q' and q_1 and a "subpolygon" between q_2 and q'. Now we can easily choose the one containing t.

4 Experimental Setup

We now describe how we conducted the experimental evaluation of our four implementations for geodesic shortest path algorithms.

4.1 Generating the Test Instances

Our experimental approach is as follows: given a desired number of vertices n, we generate 4–10 (pseudo)random polygons with n vertices. For this, we use a tool developed in a software project carried out under the supervision of Günter Rote at the Institute of Computer Science at Freie Universität Berlin [10]. Among others, the tool provides an implementation of the *Space Partitioning* algorithm for generating random simple polygons presented by Auer and Held [4].

Since our main focus was in validating the theoretical guarantees that where published in the literature, we opted for pseudorandomly generated polygons as our test set. This allowed us to quickly produce large input sets of varying sizes. Of course, from a practical point of view, it would also be very interesting to test our implementations on real-world examples. We leave this as a topic for a future study.

Next, we generate the set S of desired endpoints for the geodesic shortest paths. This is done as follows: for each edge e of each generated polygon, we find the incident triangle t_e of e in the constrained Delaunay triangulation of the polygon. We add the barycenter of t_e to S. In the end, the set S will have between $\lfloor n/2 \rfloor$ and $n - 2$ points. We will compute the geodesic shortest path for each pair of distinct points in S.

4.2 Executing the Tests

For each pair of points $s, t \in S$, we find the geodesic shortest path between s and t using each of the four implemented algorithms. Since the number of pairs grows quadratically in n, we restrict the tests to 1500 random pairs for all $n \geq 200$.

First, we run each algorithm once in order to assess the memory consumption. This is done by using the `get_traced_memory` function of the built-in `tracemalloc` module which returns the peak and current memory consumption—the difference tells us how much memory was used by the algorithm. Starting the memory tracing just before running the algorithm gives the correct values for the peak memory consumption. In order to obtain reproducible numbers we also disable Python's garbage collection functionality using the built-in `gc.disable` and `gc.enable` functions.

After that, we run the algorithm between 5 and 20 times, depending on how long it takes. We measure the processor time for each run with the `process_time` function of the `time` module which gives the time during which the process was active on the processor in user and in system mode. We then take the median of the times as a representative running time for this point pair.

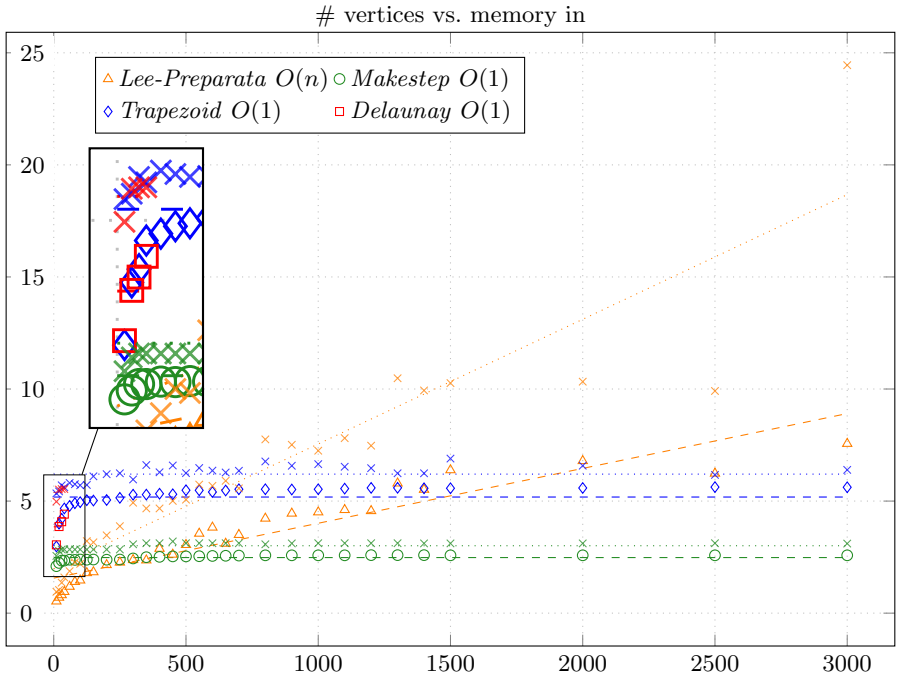

Fig. 7: Memory consumption for random instances. The outlined shapes are the median values; the semi-transparent crosses are maximum values.

4.3 Test Environment

Since we have a quadratic number of test cases for each instance, our experiments take a lot of time. Thus, the tests were distributed on multiple machines and on multiple cores. We had six computing machines at our disposal, each with two quad-core CPUs. Three machines had Intel Xeon E5430 CPUs with 2.67 GHz; the other three had AMD Opteron 2376 CPUs with 2.3 GHz. All machines had 32 GB RAM, even though, as can be seen in the next section, memory was never an issue. The operating system was a Debian 8 and we used version 3.5 of the Python interpreter to implement the algorithms and to execute the tests.

5 Experimental Results

The results of the experiments can be seen in the following plots. The plot in Figure 7 shows the median and maximum memory consumption as solid shapes and transparent crosses, respectively, for each algorithm and for each input size. More precisely, the plot shows the median and the maximum over all polygons with a given size and over all pairs of points in each such polygon.

We observe that the memory consumption for *Trapezoid* and for *Makestep* is always smaller than a certain constant. At first glance, the shape of the median

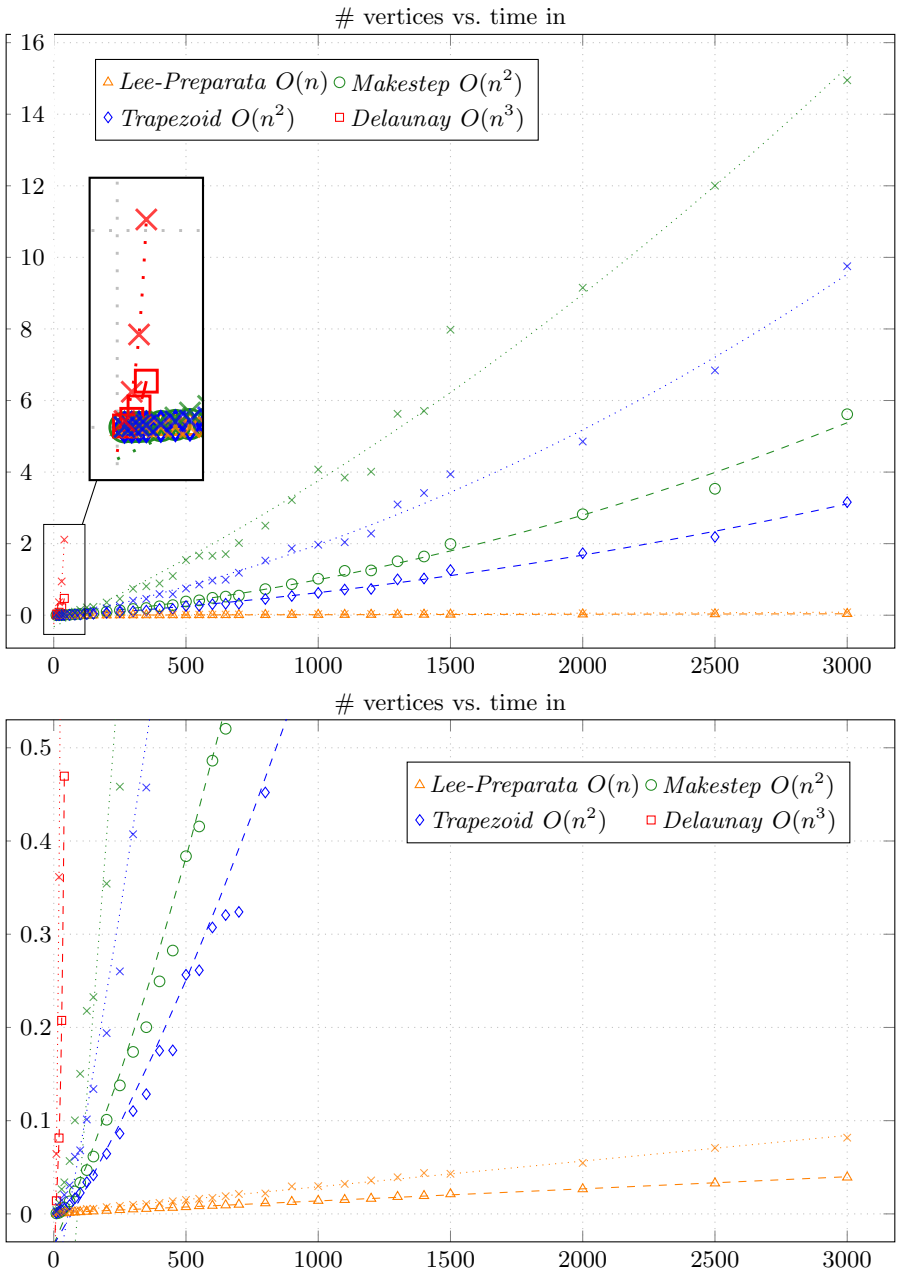

Fig. 8: Runtime for random instances. Outlined shapes are median values; semi-transparent crosses are maximum values. The bottom plot is a scaled version of the top.

values might suggest logarithmic growth. However, a smaller number of vertices leads to a higher probability that s and t are directly visible to each other. In this case, many geometric functions and subroutines, each of which requires an additional constant amount of memory, are not called. A large number of point pairs with only small memory consumption naturally entails a smaller median value. We can observe a very similar effect in the memory consumption of the *Lee-Preparata* algorithm for small values of n. However, as n grows, we can see that the memory requirement begins to grow linearly with n.

The second plot in Figure 8 shows the median and the maximum running time in the same way as Figure 7. Not only does *Delaunay* have a cubic running time, but it also seems to exhibit a quite large constant: it grows much faster than the other algorithms.

In the lower part of Figure 8, we see the same x-domain, but with a much smaller y-domain. Here, we observe that *Trapezoid* and *Makestep* both have a quadratic running time; *Trapezoid* needs about two thirds of the time required by *Makestep*. Finally, the linear-time behavior of *Lee-Preparata* can clearly be discerned.

Additionally, we observed that the tests ran approximately 85 % slower on the AMD machines than on the Intel servers. This reflects the difference between the clock speeds of 2.3 GHz and 2.67 GHz. Since the tests were distributed equally on the machines, this does not change the overall qualitative results and the comparison between the algorithms.

6 Conclusion

We have implemented and experimented with three different constant-workspace algorithms for geodesic shortest paths in simple polygons. Not only did we observe the cubic worst-case running time of *Delaunay*, but we also noticed that the constant factor is rather large. This renders the algorithm virtually useless already for polygons with a few hundred vertices, where the shortest path computation might, in the worst case, take several minutes.

As predicted by the theory, *Makestep* and *Trapezoid* exhibit the same asymptotic running time and space consumption. *Trapezoid* has an advantage in the constant factor of the running time, while *Makestep* needs only about half as much memory. Since in both cases the memory requirement is bounded by a constant, *Trapezoid* would be our preferred algorithm.

We chose Python for the implementation mostly due to our previous programming experience, good debugging facilities, fast prototyping possibilities, and the availability of numerous libraries. In hindsight, it might have been better to choose another programming language that allows for more low-level control of the underlying hardware. Python's memory profiling and tracking abilities are limited, so that we cannot easily get a detailed view of the used memory with all the variables. Furthermore, a more detailed control of the memory management could be useful for performing more detailed experiments.

References

1. Asano, T., Buchin, K., Buchin, M., Korman, M., Mulzer, W., Rote, G., Schulz, A.: Memory-constrained algorithms for simple polygons. Comput. Geom. Theory Appl. **46**(8), 959–969 (2013)
2. Asano, T., Mulzer, W., Rote, G., Wang, Y.: Constant-work-space algorithms for geometric problems. J. of Computational Geometry **2**(1), 46–68 (2011)
3. Asano, T., Mulzer, W., Wang, Y.: Constant-work-space algorithms for shortest paths in trees and simple polygons. J. Graph Algorithms Appl. **15**(5), 569–586 (2011)
4. Auer, T., Held, M.: Heuristics for the generation of random polygons. In: Proc. 8th Canad. Conf. Comput. Geom. (CCCG). pp. 38–43 (1996)
5. Baffier, J.F., Diez, Y., Korman, M.: Experimental study of compressed stack algorithms in limited memory environments. In: Proc. 17th Inter. Symp. Experimental Algorithms, (SEA). pp. 19:1–19:13 (2018)
6. Banyassady, B., Korman, M., Mulzer, W.: Computational geometry column 67. SIGACT News **49**(2), 77–94 (2018)
7. de Berg, M., Cheong, O., van Kreveld, M., Overmars, M.: Computational Geometry. Theory and Applications. Springer-Verlag, 3rd edn. (2008)
8. Chazelle, B.: Triangulating a simple polygon in linear time. Discrete Comput. Geom. **6**, 485–524 (1991)
9. Chew, L.P.: Constrained Delaunay triangulations. Algorithmica **4**, 97–108 (1989)
10. Dierker, S., Ehrhardt, M., Ihrig, J., Rohde, M., Thobe, S., Tugan, K.: Abschlussbericht zum Softwareprojekt: Zufällige Polygone und kürzeste Wege (2012), https://github.com/marehr/simple-polygon-generator, Institut für Informatik, Freie Universität Berlin
11. Ghosh, S.K.: Visibility algorithms in the plane. Cambridge University Press (2007)
12. Har-Peled, S.: Shortest path in a polygon using sublinear space. J. of Computational Geometry **7**(2), 19–45 (2016)
13. Hunter, J.D.: Matplotlib: A 2D graphics environment. Computing in Science & Engineering **9**(3), 90–95 (2007)
14. Lee, D.T., Preparata, F.P.: Euclidean shortest paths in the presence of rectilinear barriers. Networks **14**(3), 393–410 (1984)
15. Python Software Foundation: Python, https://www.python.org/, version 3.5
16. Rufat, D.: Python Triangle (2016), http://dzhelil.info/triangle/, version 20160203
17. Shewchuk, J.R.: Triangle: Engineering a 2D quality mesh generator and Delaunay triangulator. In: Workshop on Applied Computational Geormetry, Towards Geometric Engineering (WACG). pp. 203–222 (1996)
18. Tantau, T.: Logspace optimization problems and their approximability properties. Theoret. Comput. Sci. **41**(2), 327–350 (2007)

A Tables of Experimental Results

Here we list the experimental results shown in Figs. 7 and 8.

Table 1: The median and maximum memory usage in bytes for all runs with a specific number of vertices n.

	Delaunay		*Lee-Preparata*		*Makestep*		*Trapezoid*	
n	median	max	median	max	median	max	median	max
10	3048	4976	528	952	2096	2552	2976	5344
20	3864	5512	696	1032	2240	2776	3992	5432
30	4080	5536	808	1360	2344	2840	4208	5704
40	4416	5536	952	1592	2344	2840	4672	5616
60			1184	1872	2384	2840	4784	5808
80			1400	2264	2376	2840	4904	5752
100			1464	2200	2392	2840	4952	5704
125			1792	3216	2384	2840	5040	5720
150			1832	3160	2392	2840	5024	6104
200			2152	3472	2384	2840	5048	6200
250			2264	3880	2392	2840	5144	6240
300			2376	4928	2440	3072	5284	5964
350			2360	4672	2496	3120	5288	6608
400			2880	4672	2512	3120	5328	6284
450			2616	5008	2532	3200	5304	6588
500			3048	5064	2532	3120	5484	6248
550			3552	5736	2540	3120	5480	6476
600			3824	5680	2552	3120	5404	6360
650			3104	5904	2560	3120	5472	6276
700			3496	5568	2568	3120	5528	6352
800			4224	7752	2580	3072	5528	6768
900			4448	7512	2580	3112	5516	6576
1000			4504	7248	2580	3120	5528	6648
1100			4608	7808	2580	3120	5556	6532
1200			4560	7472	2588	3120	5588	6468
1300			5792	10 480	2588	3120	5592	6240
1400			5512	9936	2588	3112	5572	6240
1500			6384	10 264	2580	3112	5572	6896
2000			6792	10 328	2580	3112	5584	6580
2500			6232	9912	2580	3120	5624	6168
3000			7560	24 448	2580	3104	5616	6392

Table 2: The median and maximum running times in seconds for all runs with a specific number of vertices n.

	Delaunay		*Lee-Preparata*		*Makestep*		*Trapezoid*	
n	median	max	median	max	median	max	median	max
10	0.014 019	0.064 309	0.000 367	0.000 910	0.000 519	0.004 162	0.000 820	0.002 603
20	0.081 347	0.361 370	0.000 616	0.001 613	0.001 156	0.011 853	0.002 010	0.007 343
30	0.207 516	0.943 375	0.000 830	0.002 879	0.003 319	0.026 406	0.003 655	0.014 552
40	0.469 530	2.112 217	0.001 045	0.002 166	0.006 867	0.033 851	0.005 716	0.020 334
60			0.001 399	0.002 918	0.013 428	0.056 691	0.009 516	0.030 625
80			0.001 756	0.003 444	0.024 055	0.100 309	0.016 658	0.061 326
100			0.002 056	0.004 030	0.033 428	0.150 279	0.022 560	0.068 170
125			0.002 501	0.005 372	0.046 976	0.217 762	0.033 954	0.101 315
150			0.002 888	0.005 534	0.061 505	0.232 505	0.041 352	0.133 888
200			0.003 576	0.007 240	0.100 989	0.354 232	0.064 532	0.193 956
250			0.004 321	0.008 537	0.137 829	0.458 281	0.086 141	0.260 132
300			0.005 073	0.009 685	0.173 749	0.739 960	0.110 249	0.407 216
350			0.005 579	0.010 597	0.200 256	0.808 604	0.128 425	0.457 386
400			0.006 372	0.011 761	0.249 399	0.887 698	0.175 070	0.589 235
450			0.006 710	0.013 537	0.282 497	1.096 251	0.175 412	0.587 010
500			0.007 469	0.015 005	0.383 682	1.541 501	0.256 470	0.746 144
550			0.008 528	0.016 190	0.415 579	1.666 938	0.261 306	0.859 130
600			0.008 899	0.017 127	0.486 157	1.660 158	0.307 261	0.969 043
650			0.009 350	0.018 987	0.520 370	1.707 651	0.320 547	0.991 330
700			0.010 033	0.021 339	0.548 668	2.018 272	0.323 926	1.187 180
800			0.011 583	0.021 906	0.729 638	2.502 922	0.452 032	1.526 597
900			0.012 974	0.029 481	0.866 354	3.218 503	0.536 978	1.866 497
1000			0.014 204	0.029 770	1.019 635	4.070 813	0.623 762	1.969 603
1100			0.015 121	0.032 160	1.239 577	3.846 221	0.717 239	2.040 144
1200			0.016 401	0.035 842	1.251 472	4.010 515	0.733 767	2.282 640
1300			0.018 357	0.039 272	1.506 918	5.627 138	1.001 474	3.095 028
1400			0.019 354	0.043 886	1.641 150	5.707 774	1.026 240	3.415 236
1500			0.021 279	0.043 013	1.990 088	7.978 124	1.261 539	3.941 024
2000			0.026 627	0.054 653	2.821 684	9.151 548	1.731 935	4.854 338
2500			0.032 861	0.070 760	3.533 656	12.003 607	2.187 277	6.840 824
3000			0.039 188	0.081 773	5.616 593	14.949 720	3.159 590	9.751 315